

# Design of Rapid Impact Compaction at the New Yogyakarta International Airport

M. Sams

Geotechnical Engineer, Geoinventions Consulting Services Pty Ltd, Brisbane, AUSTRALIA  
[info@geoinventions.com.au](mailto:info@geoinventions.com.au)

W. He

Geotechnical Engineer, Geoinventions Consulting Services Pty Ltd, Brisbane, AUSTRALIA  
Changsha University of Science and Technology, Changsha, CHINA  
[info@geoinventions.com.au](mailto:info@geoinventions.com.au)

J. Gamaliel

Geotechnical Engineer, Geoinventions Consulting Services Pty Ltd, Brisbane, AUSTRALIA  
[info@geoinventions.com.au](mailto:info@geoinventions.com.au)

M. Mueller

Engineering Manager, Vantage Commerce Pte. Ltd, Singapore, SINGAPORE  
[m.mue@vantage-commerce.com](mailto:m.mue@vantage-commerce.com)

B. Kok

Technical Director, Geoinventions Consulting Services Pty Ltd, Brisbane, AUSTRALIA  
[info@geoinventions.com.au](mailto:info@geoinventions.com.au)

## ABSTRACT

Rapid Impact Compaction has been adopted as part of the ground improvement works to mitigate potential seismic liquefaction at the New Yogyakarta International Airport. The surface soil material vulnerable to liquefaction is comprised of up to eight metres of very loose to loose sand, typical to the coastal areas of the region. The design of the ground improvement has been conducted using finite element modelling and the soil composite block approach. In the FEM, the dynamic loading of the compaction is modelled with the existing soil, and the influence area of improvement can be predicted. With the composite block approach, the geotechnical parameters of the block are required to correlate to the SPT and CPT requirements to mitigate liquefaction. Based on this, a design spacing of  $S/D=1.17$  was stipulated, with two phases and two cycles. A trial of this design configuration has been conducted on site with CPT and SPT testing, to demonstrate the effectiveness of the design. This has indicated substantial improvement from the initial state to the first compaction cycle, and reduced improvement from the first cycle to the second cycle. In terms of SPT results, a 200-300% improvement at the surface and 20-43% improvement at 8m depth was measured. An preliminary empirical design methodology has developed based on the test results. With future testing and further development of the numerical modelling, this can form a robust and optimised design approach for rapid impact compaction.

**Keywords:** rapid impact compaction, liquefaction, airport, soil composite block.

## 1 INTRODUCTION

Ground improvement is often a significant part of large construction projects in regions with unfavourable ground conditions. This is especially the case in many parts of south-east Asia where the active seismic conditions become more dominant in the geotechnical engineering design.

Indonesia is particularly seismically active, with several substantial seismic events per year. For the geotechnical designer, this has a number of

implications. For the loose iron sands along the south of the Java island, liquefaction is a project risk to be addressed by the designer.

As part of a wider effort to increase tourism for Yogyakarta and the surrounding region, a new international airport is to be constructed approximately 40km south-west of Yogyakarta city. This New Yogyakarta International Airport (NYIA) will have a 3.6km runway and full terminal facilities that have a footprint of up to 107,000m<sup>2</sup>.

The existing ground has been deemed a liquefaction risk by the designer. Therefore, ground improvement was required to sufficiently mitigate the potential for liquefaction. The design criteria to achieve this improvement is summarised in Table 1. These comprise of Standard Penetration Tests (SPTs), Cone Penetration Tests (CPTs), and Relative Density ( $Dr$ ).

Table 1. Acceptance criteria for ground improvement

Depth (m)	SPT-N	CPT - $q_c$ (MPa)	$Dr\%$ (Relative Density)
2	16	7	>70
4	22	9	>70
6	26	13	>70
8	30	15	>70

Rapid Impact Compaction (RIC) was selected as the ground improvement method for the terminal area. This was due to the sand ground conditions and required improvement depth in the ideal range of RIC. This machine uses a high frequency, low drop height hammer to achieve the compaction. A photograph of the RIC machinery is shown in Figure 1. This RIC attachment is comprised of a 9t hammer & 4t foot.



Figure 1. RIC attachment mounted on excavator

The methodologies to determine the degree of improvement are rare and often are only specific to each project. In addition to this, they are often based on the composite block approach. This is due to the difficulty of this three-dimensional, dynamic problem and the number of variables that impact the result. These include: initial ground conditions, fines (<0.075mm) content, impact energy of the machinery, spacing, depth of improvement, water table level.

The outcome for the designer is required to be the geometry configuration (RIC diameter  $D$ , and spacing

$S$ ), and termination criteria for the machine. The design of the ground improvement for the NYIA required a diameter of 1.5m, primary spacing of 3.5m, and overall spacing after secondary phase of 1.75m. See Figure 2 for an illustration of the spacing. The termination criteria used were:

- a) Maximum cumulative deflection of 1000mm
- b) Minimum deflection per blow of 10mm
- c) Maximum number of blows per column of 60

The purpose of this paper is to document the design process that has been adopted, and the outcomes of a RIC trial that has been undertaken on-site. In addition to this, the difficulties and limitations of the design process are discussed, with suggested future work to develop a reliable design method.

## 2 DESIGN METHODOLOGY

A typical diagram of the design problem is shown in Figures 2 and 3. As discussed, the effectiveness of the RIC is a function of: initial soil conditions, spacing ratio ( $S/D$ ), and the compaction energy (hammer weight, drop height). In the design case, the initial soil conditions can be assumed constant (i.e worst case conditions), and the compaction energy can remain constant (consistent machinery and operation). Therefore, the objective of the design is determining the required spacing ratio.

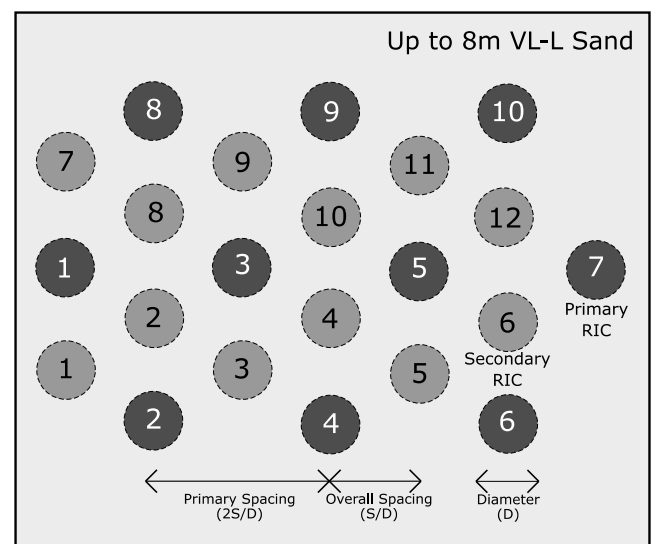


Figure 2. Typical plan view of the RIC design problem

Design of the RIC ground improvement has been undertaken using a combination of numerical modelling and conventional empirical method. The numerical modelling is conducted using finite element analysis with ABAQUS v6.12 (Dassault Systèmes Simulia, 2014). The conventional empirical method uses a composite soil block approach.

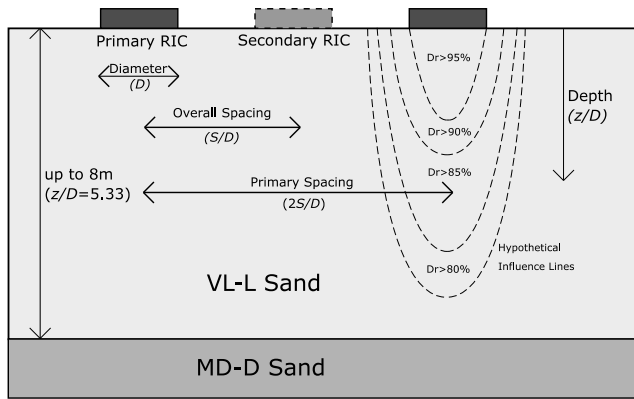


Figure 3. Typical side view of the design problem

Using these approaches the spacing of the RIC columns can be determined to achieve the required improvement to the vulnerable layer of soil. Following the design analysis, a trial has been conducted to verify the design configuration. This also allows the designer to collect data for design/model calibration and future design optimisation.

The design process has generally followed the following process:

- a) Step 1 - The soil composite block approach is used to find the RIC spacing required to meet SPT-N requirements.
- b) Step 2 - The numerical modelling is used to determine confirm that the influence area of the proposed spacing is appropriate.
- c) Step 3 - A trial of the proposed RIC configuration with SPT and CPT is conducted on site to assess the performance of the design configuration.
- d) Step 4 - If the performance of the RIC is substantially different than predicted, a back analysis is to be conducted to find the errant input parameter/s.

### 3 SOIL COMPOSITE BLOCK APPROACH

The soil composite block approach has been used in ground improvement for decades as a convenient and intuitive way of accounting for the spacing and the initial ground conditions. In particular, the design methodology documented by Goughnour et al (1991) and Poulos (2002) has been followed.

This approach allows the designer to treat the improved ground layer as one homogenous block. Design parameters are calculated using a weighted average of based on the proportion of each of the component materials. In this approach, the ground improvement by RIC is assumed to act as columns with diameter  $D$ .

Using this approach, the design parameters (unit weight and friction angle) of the equivalent soil block must correlate to the SPT-N criteria required for the liquefaction mitigation. Therefore, the spacing of the RIC columns can be adjusted until this requirement is met. The input parameters for the existing ground and RIC ‘column’ materials are as shown in Table 2.

Table 2. Acceptance criteria for ground improvement

Material	Unit Weight (kN/m <sup>3</sup> )	Young’s Modulus (MPa)	Effective Friction Angle (deg)
Existing Ground	18	10	28
RIC ‘Columns’	22	50	35

The parameters of the equivalent block can be calculated using Equation (1) and (2), where  $A$  can be the following: unit weight  $\gamma$ , effective cohesion  $c'$ , and effective friction angle  $\tan(\phi)$ .  $k$  is the improved area ratio. Equations (1) and (2) have been found to consistently underestimate Young’s Modulus  $E$ . Therefore, this can be estimated using Equations (3) and (4), where  $k_E$  is the modified area ratio, using the pattern coefficient  $\zeta$ . The calculated composite block parameters for a range of  $S/D$  are shown in Figure 4.

$$A_{composite} = kA_{RIC} + (1 - k)A_{soil} \quad (1)$$

$$k = \frac{\pi D^2}{4S^2} \quad (2)$$

$$E_{composite} = E_{RIC} \left( k_E + \frac{E_{soil}}{E_{RIC}} \right) (1 - k_E^2) \quad (3)$$

$$k_E = \zeta \left( \frac{D}{S} \right)^2 \quad (4)$$

$$\zeta = 0.78 \text{ (square)}, \zeta = 0.91 \text{ (triangular)}$$

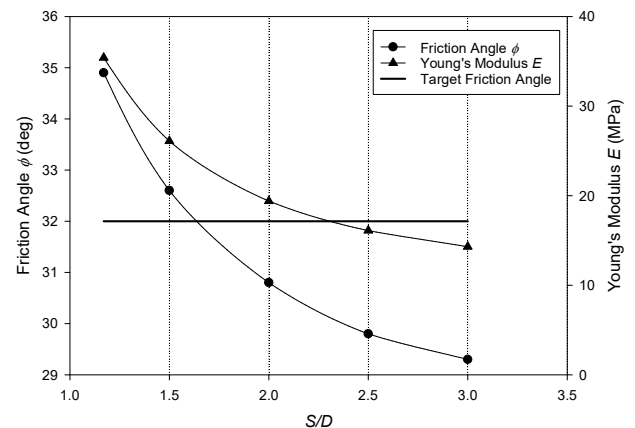


Figure 4. Estimated Parameters of Composite Block

The improved ground is required to achieve an SPT-N value of at least 16, as per Table 1. This has been correlated to friction angle using Equation (5), from Peck, Hanson, & Thornburn (1974). Using Equation (1), an SPT-N of 16 correlates to a friction angle of approximately 32 degrees. The ground improvement composite block is required to achieve this friction angle.

$$\phi' = 27.1 + 0.3N_{60} - 0.00054N_{60}^2 \quad (5)$$

This requirement has been shown in Figure 3 as the ‘Target’ line. This indicates that the overall spacing ratio is required to be less than 1.6.

#### 4 NUMERICAL MODELLING OF RIC

The RIC has been modelled with finite element analysis in the ABAQUS software. A simplified 2D plane strain approach is used, similar to that shown in Figure 3. Three RIC impact sites are modelled - two primary which occur first and one secondary which occurs last. The soil material is simulated using a

strain hardening model. The boundary conditions on the base and sides are modelled with infinite elements.

The dynamic loading caused by the hammer drop is modelled using a repeating surcharge with time function. This function is developed based on the expected hammer drop frequency of the machinery. Using a 9t hammer and a 1.2m drop height, a surcharge of 135kN is applied for 0.1 second, every second. The surcharge is assumed to increase from zero to peak and back to zero in 0.1s.

A number of models have been assessed with the overall *S/D* varying from 1.17, 1.5, and 2. The surcharge application and initial soil conditions have been kept constant. The contour charts of equivalent plastic strain (PEEQ) for each *S/D* case are shown in Figure 5. This represents the influence area of the compaction, similar to the research by Gu and Lee (2002). Note that the each model is 10m high. As expected, the maximum influence is at the base of the surcharge and extends down in a bulb shape.

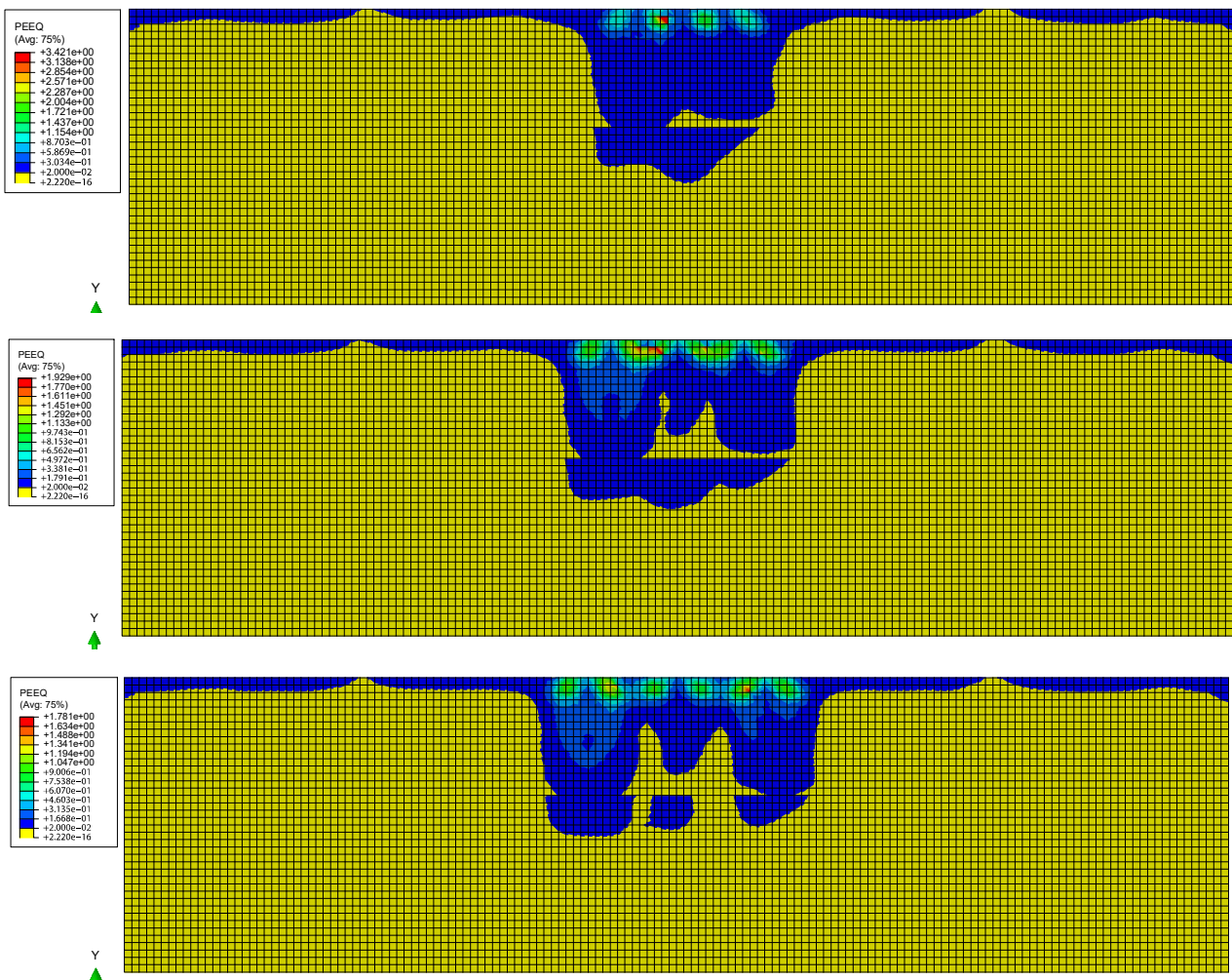


Figure 5. Equivalent plastic strain (PEEQ) contour charts for *S/D*=1.17 (top), *S/D*=1.5 (middle), *S/D*=2 (bottom). Note that the height of model is 10m

These results indicate that substantial improvement extends to depths of up to 6m. In the  $S/D=1.17$  case, the improvement is almost constant to this 6m depth. In the  $S/D=2$  case, there is substantial gaps in the influence zone between the columns at 3-6m depth. At  $S/D=1.5$ , these gaps are relatively minor and may not have a significantly adverse impact on the outcome. However, the impact of this is still unclear. Overall, the results of the numerical modelling are consistent with the outcome of the composite block approach, in recommending an  $S/D < 1.6$ .

### 5 ON-SITE RIC TRIAL

Based on the outcomes of the numerical and empirical assessment, a design configuration was proposed comprising 1.5m diameter RIC columns with an overall 1.75m spacing in a triangular pattern. This was achieved with a primary stage using 3.5m spacing in a triangular pattern, and a secondary stage that placed an RIC column in the centre of each 3.5m triangle.

As part of the design process, an on-site trial was specified to verify the performance of the RIC configuration. This trial was conducted using two cycles of the primary and secondary stages. SPT testing was conducted prior to, and after each cycle. CPT testing was conducted before testing and after cycle 2. The adopted RIC configuration and testing is indicated in Figure 6.

The results of the SPT testing have been summarised in Table 5. The SPT and CPT test results are shown in Figures 7 and 8. Note that the test numbers (*SPT3*, *CPT2* etc) are shown in Figure 6. The project acceptance criteria have been shown for this testing.

This testing shows a substantial improvement from the initial state to after the RIC.

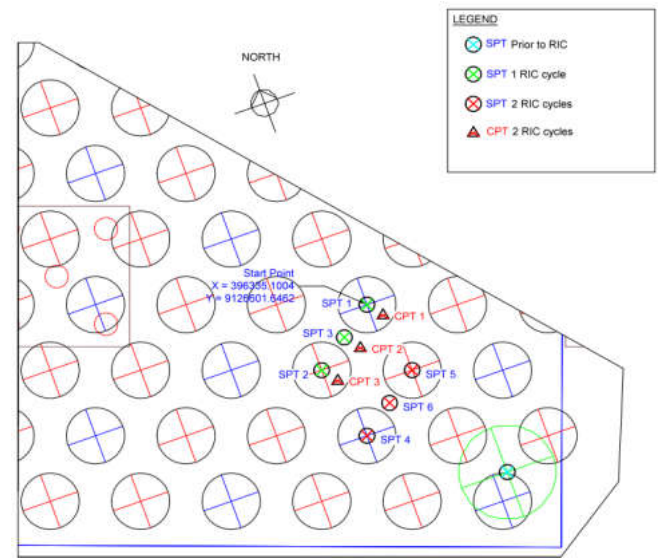


Figure 6. Configuration for the RIC trial

In terms of the SPT scores, the degree of improvement after the first cycle is  $>250\%$  at 2m depth, and reduces with depth. Further improvement occurs during cycle 2, but on a reduced scale. This is summarised in Table 3.

Note that at 6m depth, the improvement from ‘initial to cycle 2’ is lower than ‘initial to cycle 1’, indicating that the SPT conducted after cycle 2 yielded a lower result than after cycle 1. This can also be observed in Figure 7 - ‘Between Columns’. It is expected that this is due to the inherent variability and inaccuracy of the SPT testing, and a statistically low number of tests.

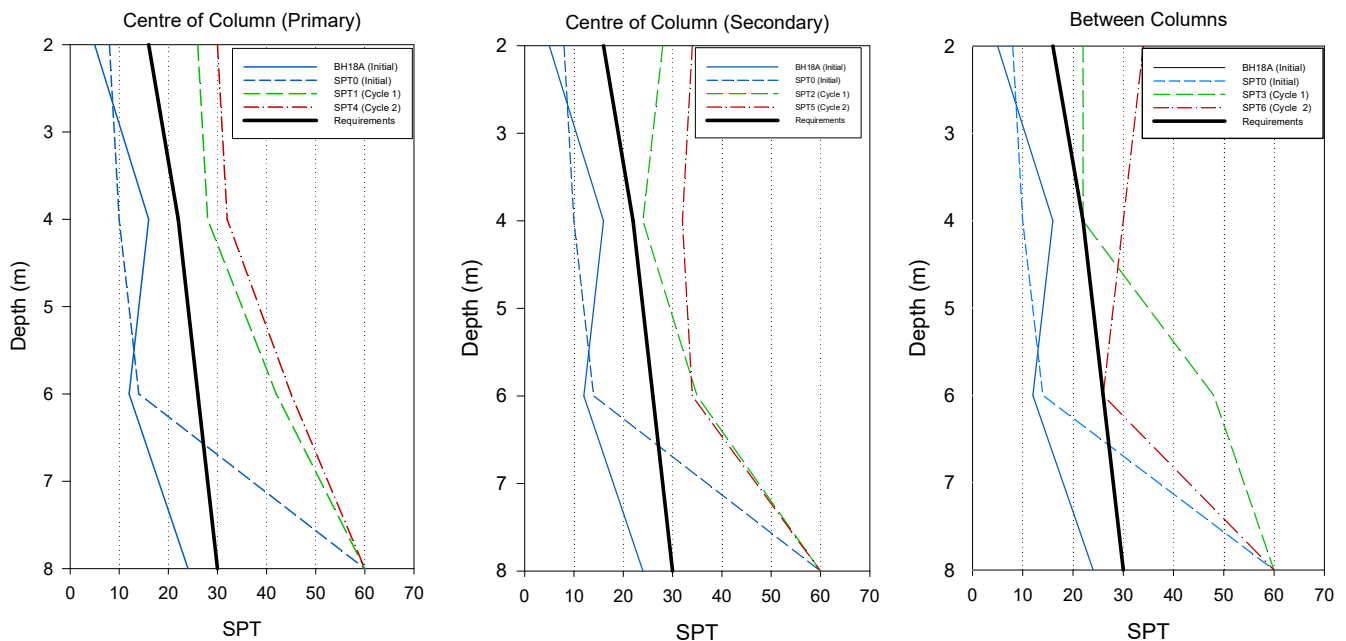


Figure 7. SPT results at each location for all cycles

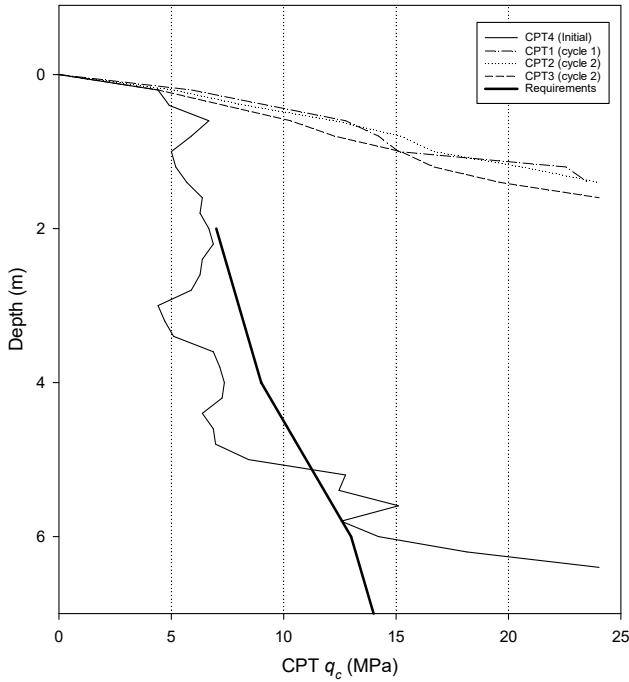


Figure 8. Results of the CPT testing

All SPT results, regardless of position, have been graphed against depth in Figure 9. A logarithmic line of best of fit is shown. This graph demonstrates the overall trend of improvement due to RIC. That is, there is dramatic improvement from the initial state to cycle 1, and a reduced improvement from cycle 1 to cycle 2. The degree of improvement gradually reduced with depth, but is still evident even at 8m depth.

Table 3. Average degree of improvement in terms of SPT

Depth (m)	Initial to Cycle 1	Initial to Cycle 2
2	289.7%	402.6%
4	89.7%	141%
6	220.5%	169.2%
8	42.9%	42.9%

The improvement observed in cone resistance ( $q_c$ ) from the CPTs, as shown in Figure 8, is also substantial. As the tests were limited to a 2.5t CPT, these all encountered refusal before 2m depth.

Table 4. Summary of the SPT Results for the RIC Trial

Depth (m)	SPT Required	Cycle 0 (Initial)		Cycle 1			Cycle 2		
		BH18A	SPT0	SPT1	SPT2	SPT3	SPT4	SPT5	SPT6
2	16	5	8	26	28	22	30	34	34
4	22	16	10	28	24	22	32	32	30
6	26	12	14	42	35	48	34	34	26
8	30	24	>60	>60	>60	>60	>60	>60	>60

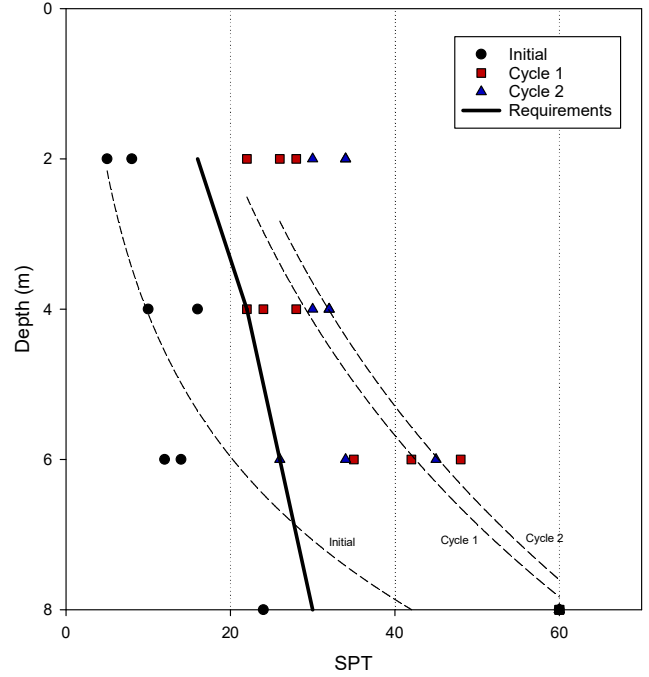


Figure 9. Overall trend of the SPT results

## 6 BACK-CALCULATED DESIGN METHODOLOGY FOR SOUTH JAVA IRON SANDS

Following the on-site trial of the RIC, further analysis of the testing results has been conducted. This has been used to determine a preliminary method for the design of RIC in South Java iron sands.

The design of RIC will generally require achieving SPT and CPT targets, such as those criteria in Table 1 for the project discussed in this paper. Therefore, the design methodology of RIC must be able to predict the SPT results ( $SPT_{final}$ ) following the RIC treatment, based on information that will typically be available at the design stage. This includes SPT testing at the initial condition ( $SPT_{initial}$ ), distance (from the centre of RIC column) ratio ( $s/D$ ), and depth ratio ( $z/D$ ). This can be summarised, as in Equation (5).

$$SPT_{final} = f\left(SPT_{initial}, \frac{s}{D}, \frac{z}{D}\right) \tag{5}$$

In Figure 10, all SPTs are graphed against the correspondingly positioned SPT in the preceding RIC cycle. So, in the cycle 1 stage - the cycle 1 SPTs are 'final' and the SPTs at the initial state are 'initial'. In the cycle 2 stage - cycle 2 SPTs are 'final' and the SPTs from cycle 1 are 'initial'. The solid line is 1V:1H, which represents where the initial and final SPTs are equal.

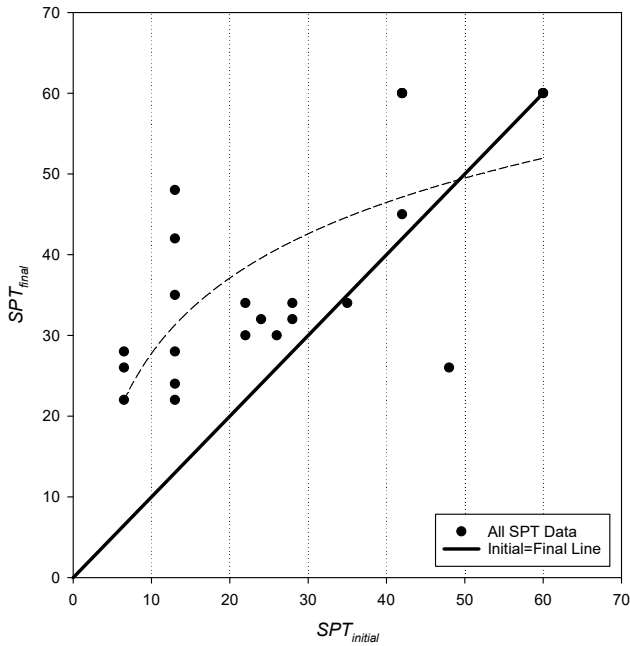


Figure 10. Initial SPT against final SPT results

Results that fall below this line indicate that the SPT result is lower than from the previous cycle, a condition which should not occur. Thus, it is logical that all points should be above the line; the further above the line the higher the degree of improvement.

The chart shows that the degree of improvement is high when the initial SPT is low, and reduces as the initial SPT increases. The data points have been fitted with a logarithmic line, as this is found to be the best fit, the regression equation and fit coefficient are shown. Based on this regression, the general equation for  $SPT_{final}$  can be expressed as in Equation (6), where the  $\alpha$ ,  $k$  and  $c$  coefficients are dependant on  $s/D$  and  $z/D$ .

$$SPT_{final} = \alpha [k \ln(SPT_{initial}) + c] \quad (6)$$

$$k = -2.43 \frac{z}{D} + 10.5 \quad (7)$$

$$c = 14.47 \frac{z}{D} - 15.4 \quad (8)$$

Figure 11 is a reproduction of Figure 10, with the data points separated by the depth of the test. Based on this,

the  $k$  and  $c$  coefficients are found to be related to  $z/D$  by Equations (9) and (10) respectively.

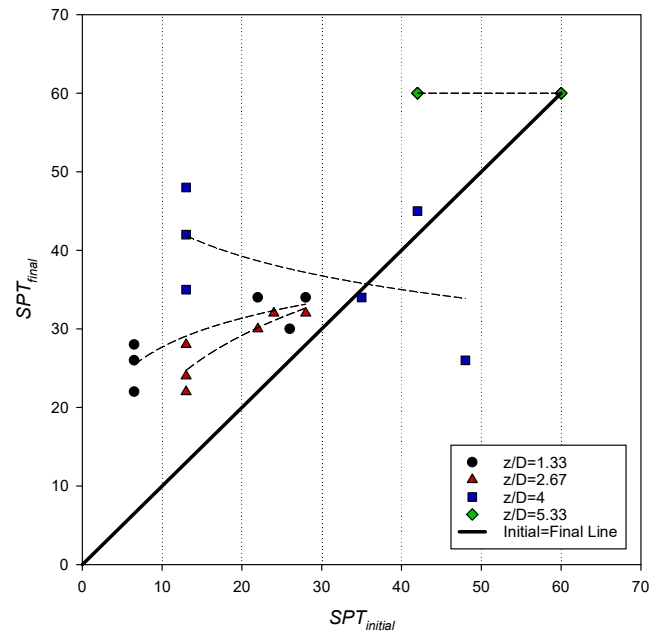


Figure 11. Initial SPT against final SPT results, separated by depth

Using Equations (6), (7), and (8), the contour chart, Figure 12, has been generated that allows the user to estimate  $SPT_{final}$  based on  $SPT_{initial}$  and the depth ratio ( $z/D$ ). For example, the post-RIC SPT can be estimated at  $z/D=2$ . If the initial SPT ( $SPT_{initial}$ ) is 15, then the estimated post-RIC SPT value ( $SPT_{final}$ ) is estimated to be 28. Note that the red shaded area indicates where  $SPT_{initial}$  is less than  $SPT_{final}$ , which should be an invalid result.

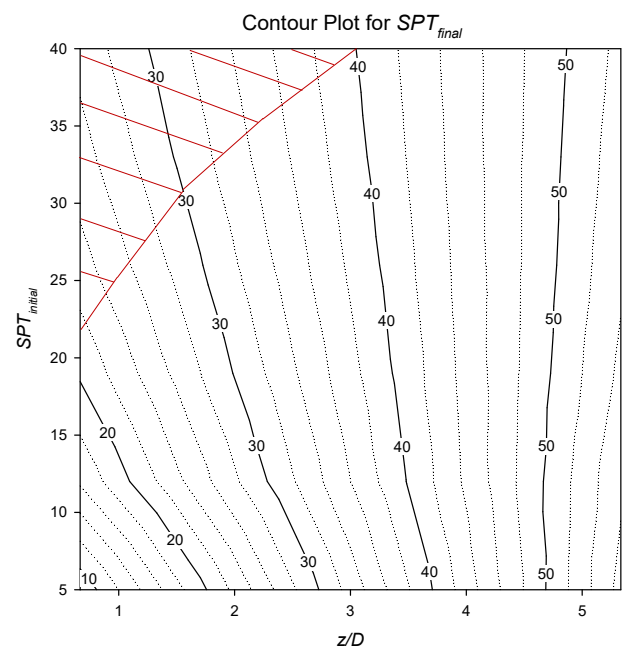


Figure 12. Contour Chart to estimate Post-RIC SPT values

Note that the estimate provided using Figure 12 is only applicable directly beneath the RIC columns. The post-RIC SPT result can also be expected to reduce between the columns. Thus, the spacing reduction factor  $\alpha$ , as shown in Figure 13, can be used to suitably reduce the result from Figure 12 based on the distance ratio from the centre of the RIC column  $s/D$ . Continuing the previous example, the user can predict the spacing reduction factor at  $s/D=1$ . In this instance,  $\alpha=0.9$ . Therefore, the estimated  $SPT_{final}$  using Figures 12 and 13 at  $z/D=2$ ,  $s/D=1$  is 25.2.

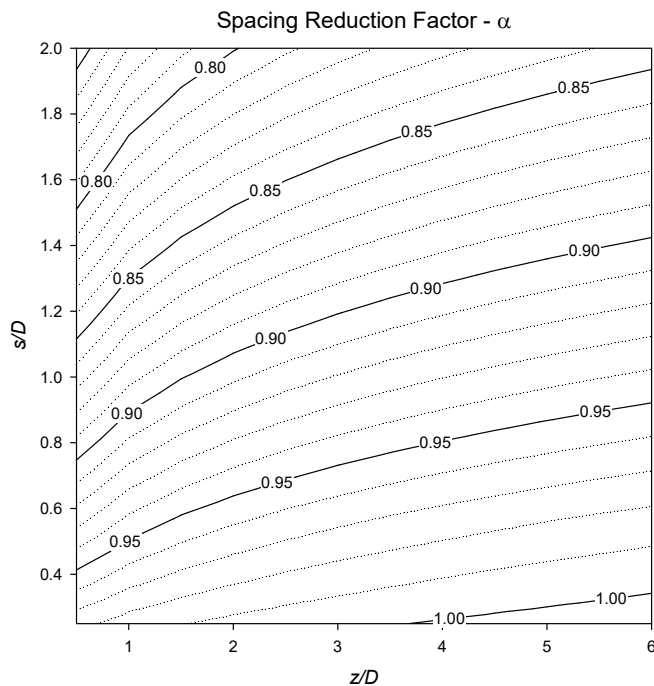


Figure 13. Contour plot for spacing reduction factor  $\alpha$

## 7 CONCLUSION

Using the soil composite block approach, the spacing ratio is required to be less than 1.6 to achieve the material criteria. The results of the numerical modelling indicated that the likely upper limit of the spacing ratio was 1.5. Based on this, the design and the RIC trial conducted on site used a spacing ratio of 1.17.

The results of the trial exceeded expectations with improvement of greater than 200% measured in the first 4m, and up to a 42% to 8m depth, in terms of SPT value. The CPT tests also measured a substantial improvement, with cone resistance increasing by several multiples.

The soil composite block is a simple design approach that can take into account a number of the important parameters and provides a good estimate of the spacing. However, it is very basic approach that is ineffective at analysing a layered soil profile, and

provides no indication of the depth of improvement. In addition to this, a number of assumptions are required by the designer including the analytical treatment of RIC as perfect columns and the corresponding design parameters of these columns.

Therefore, a numerical modelling approach is under development to provide a more robust design solution, which can take into account more of the required inputs and provide an optimised solution. It is noted that RIC is inevitably a three dimensional process. Therefore the 2D plane strain modelling will likely produce an aggressive result, as the pressure is overestimated as a strip load, and the impact energy only gets dissipated laterally, and not three dimensionally as in the real case. In addition to this, 2D axisymmetric models are unable to simulate the spacing and staging of the RIC.

The results of real project testing are being used to develop a back-calculated empirical design methodology. Note that this approach has only taken data from the trial at NYIA with the corresponding machine and soil conditions. Thus, it is likely only applicable with similar conditions.

RIC is concluded to be a very effective ground improvement method when used in sandy material, as at the NYIA and the South Java iron sands generally.

## REFERENCES

- Dassault Systèmes Simulia, 2014. Abaqus 6.12 Analysis User's Guide.
- Goughnour, R. R., Sung, J. T., & Ramsey, J. S. (1991). Slide correction by stone columns. In *Deep Foundation Improvements: Design, Construction, and Testing*. ASTM International.
- Gu, Q. and Lee, F.H., 2002. Ground response to dynamic compaction of dry sand. *Geotechnique*, 52(7), pp.481-493.
- Peck, R.B., Hanson, W.E. and Thornburn, T.H., 1974. *Foundation engineering* (Vol. 10). New York: Wiley.
- Poulos, H.G. (2002), *Research Report on Foundation Design for Very Soft Clays*, Coffey's Technical Innovation Group.